Locating enzyme activities and nutrients in the rhizosphere: Combining zymography and DET methods

Louise Paillat, Patrice Cannavo, Aurélia Mouret, Édouard Metzger, L. Huché-Thélier, F. Barraud, Ahmad Samir Azimi, J Cardenas, Banfield C, Yakov Kuzyakov, et al.

Soil Biology and Biochemistry 213 (2026) 110039

Contents lists available at ScienceDirect

Soil Biology and Biochemistry

journal homepage: www.elsevier.com/locate/soilbio

Locating enzyme activities and nutrients in the rhizosphere: Combining zymography and DET methods

L. Paillat [a,b], P. Cannavo [a,*], A. Mouret [c], E. Metzger [c], L. Huché-Thélier [d], F. Barraud [b], A.S. Azimi [e], J. Cardenas [f], C. Banfield [g], Y. Kuzyakov [h,i], M. Dippold [g], R. Guénon [a]

[a] EPHOR, Institut Agro, 49045, Angers, France
[b] PREMIER TECH GHA SAS, Le Ciron, 49680, Vivy, France
[c] Univ Angers, Nantes Université, Le Mans Université, CNRS, Laboratoire de Planétologie et sciences, LPG UMR 6112, 49000, Angers, France
[d] Univ Angers, Institut Agro, INRAE, IRHS, SFR QUASAV, 49000, Angers, France
[e] Biogeochemistry of Agroecosystems, Department of Crop Science, University of Göttingen, Göttingen, Germany
[f] Facultad de Ciencias Agropecuarias y Recursos Naturales, Grupo de Investigación Innovación en Sistemas Agrícolas y Forestales (ISAF), Universidad de los Llanos, Villavicencio, Colombia
[g] Geosphere-Biosphere Interactions, Department of Geosciences, University of Tübingen, Tübingen, Germany
[h] Department of Soil Science of Temperate Ecosystems, Department of Agricultural Soil Science, University of Goettingen, Göttingen, Germany
[i] Peoples Friendship University of Russia (RUDN University), Moscow, Russia

ARTICLE INFO

Keywords:
Mapping
Soil
Peat soil
Carbon
Nitrogen
Phosphorus cycling
Rhizobox

ABSTRACT

Organic fertilization is a recognized sustainable practice in agriculture and represents a major nutrient source for microbes and plants in these systems. Microbes produce hydrolytic enzymes to mineralize nutrients from organic forms into mineral forms to satisfy their own needs, and thus can compete with plants for these mineralized nutrients. Thus, interactions between plants and microbes in the rhizosphere determine nutrient availability and flows. We investigated these relations, using a spatial approach that combined zymography with the method of diffusive equilibrium in thin films (DET) to localize enzyme activity and N and P availabilities simultaneously. Basil (*Ocimum basilicum* L.) was grown in rhizoboxes filled with an organo-mineral crop soil (MS) or 100 % organic peat soil (OS) that was unfertilized or fertilized locally with horn meal for 20 days. In general, enzyme activities were higher in MS than in OS, but the stimulation of leucine aminopeptidase (LAP) activity and associated decrease in nutrient availability was 2 times as strong in OS as in MS. A rhizosphere effect, in which rhizodeposits stimulated enzyme activity, was clearly observed in OS. Fertilization increased LAP activity and nutrient availability near the location of fertilization, which increased basil growth in OS but not in MS. β-glucosidase, acid phosphatase and N-acetyl-glucosaminidase activities responded weakly to fertilization and the rhizosphere. By relating enzyme activities mapped by zymography to nutrient availability mapped by DET, we identified microbial hotspots in the rhizosphere where most nutrient mobilization processes and competition between plants and microbes occurred.

1. Introduction

Microbes and plants establish intimate relations in soil that increase their water and nutrient uptake (Richardson et al., 2009; Chaparro et al., 2012; Pii et al., 2015), but that can also cause them to compete for nutrients (Kuzyakov and Xu, 2013). Thus, understanding plant-microbe interactions at the root–soil interface (i.e. rhizosphere) can help to increase plant productivity and environmental sustainability. The rhizosphere is the small volume of soil that surrounds roots and is one of the most dynamic habitats on Earth for the movement and storage of elements and water, oxygen (O_2) and carbon dioxide (CO_2) fluxes, microbial colonization and activities from root surfaces into the bulk soil. This volume is a major soil microbial hotspot, with high spatial and temporal heterogeneities (Hinsinger, 1998). Plant-microbe interactions are driven by their requirements for carbon (C), nutrients (mainly nitrogen (N) and phosphorus (P)) and energy, which limit their maintenance, growth and reproduction. By providing labile C through rhizodeposition, plants stimulate microbial activities involved in nutrient remobilization

* Corresponding author.
E-mail address: patrice.cannavo@institut-agro.fr (P. Cannavo).

https://doi.org/10.1016/j.soilbio.2025.110039
Received 17 July 2025; Received in revised form 12 November 2025; Accepted 14 November 2025
Available online 14 November 2025

(Nguyen, 2003). Beneficial relations tend to take over in the long term, until dynamic equilibrium is reached (Kuzyakov and Xu, 2013). However, the rhizosphere does not lie a specific distance from the root but instead consists of gradients (e.g. nutrient concentrations, microbial biomass, enzyme activities, root-derived C) from roots to the bulk soil, which represents average soil conditions (Darrah, 1993), that depends greatly on the parameter monitored (Kuzyakov and Razavi, 2019). Thus, methods for measuring nutrients and enzyme activities need to be combined to map the complex functioning of these hotspots.

In cropping systems, organic fertilizers are frequently applied to soils and take advantage of plant-microbe synergies to increase plant productivity or at least mitigate nutrient depletion caused by frequent biomass removal. To be available for plant uptake, organic forms of nutrients, such as N or P, need to be mineralized by heterotrophic microbes into mineral forms through the activity of extracellular enzymes (e.g. Caldwell, 2005; Plante et al., 2015). N released as ammonium (NH_4^+) is then converted through nitrification into nitrate (NO_3^-), the form that plants take up most rapidly (Mantelin and Touraine, 2004). Fertilization changes microbial activity locally (Kuzyakov and Blagodatskaya, 2015) and can modify the spatial distribution of plant-microbe interactions by changing C and nutrient availability (Liu et al., 2017).

Studying microbial hotspots (e.g. near roots and organic fertilization) requires non-destructive spatial identification and localization methods (Philippot et al., 2013; Kuzyakov and Blagodatskaya, 2015; Bilyera and Kuzyakov, 2024), such as in situ two-dimensional (2D) imaging (Moran and McGrath, 2021). Zymography was developed to map enzyme activities in soil, especially microbial activity that highlights specific functions, such as protease or phosphatase activity involved in mineral N and P release, respectively (Spohn et al., 2013b; Spohn and Kuzyakov, 2013). Studying microbial hotspots in soils and sediments can also be achieved by studying sub millimetric distribution of solutes through gel-based techniques such as diffusive gradients in thin films (DGT, Davison et al., 1997) or equilibrium in thin films probes (Davison et al., 1991). DET involves placing a probe gel onto a sample matrix until the gel reaches diffusional equilibrium with pore-water solutes (i.e. nutrients) (Jézéquel et al., 2007; Metzger et al., 2016). The main difference between DGT and DET is that DGT has a binding agent that will uptake the solute from porewaters inducing a release from the solid phase that can or cannot sustain the porewater concentration of the uptaken solute.

A multi-analyte solute imaging approach integrating diffusive gradients in thin films (DGT) with laser-ablation ICP-MS was successfully achieved to resolve spatial heterogeneity of nutrient availability and root-induced nutrient depletion and mobilization along individual root axes at a planar interface (Kreuzeder et al., 2018; Santner et al., 2012). More recently, DGT was combined to zymography to evaluate the distribution of phosphatase activity and labile solutes at the root–soil interface (Hummel et al., 2021). Mapping nutrients in a complex matrix using the method of diffusive equilibrium in thin films (DET) was developed for soils and sediments (Kreuzeder et al., 2013; Santner et al., 2015). However, for the first time, we adapted and simultaneously combined multiple zymography and nutrient DET imaging probes including nitrogen speciation as a novel approach to study rhizosphere processes.

To investigate effects of root-soil interactions on enzyme activities and nutrient availability, two contrasting soils were selected: an organo-mineral soil (MS) and an organic soil (OS). The MS was a cropped soil that contained active microbial communities and nutrients, while the OS was a sphagnum peat soil used in horticulture that had extremely low microbial activity (Paillat et al., 2020). This study aimed to investigate (1) plant-microbe interactions by identifying the spatial distribution of enzymes and nutrients and (2) effects of organic fertilization on these interactions in relation to C–N–P cycles. We selected four hydrolytic enzymes to cover the microbial functions involved in C–N–P cycles: 1.4-β-glucosidase (β-Glu) (one of the enzymes used most to degrade cellulose and hydrolyze glucosides and oligosaccharides into glucose), L-leucine aminopeptidase (LAP) (hydrolyzes protein into leucine and other amino acids), N-acetyl-glucosaminidase (NAG) (a chitinase involved in hydrolyzing chitin) and acid phosphatase (acid-P) (hydrolyzes organic P into phosphate (PO_4^{3-}) esters). These enzymes influence key reactions in hydrolysis during mineralization and thus contribute to mineral nutrient availability (e.g. HPO_4^{2-}, NH_4^+) directly (e.g. acid-P) or indirectly (e.g. LAP, NAG) by providing the substrates for ammonification (Sinsabaugh et al., 2008; Nannipieri et al., 2018). We used basil (*Ocimum basilicum* L.) as the plant model, since it is widely grown for ornamental, culinary and medicinal purposes (Zheljazkov et al., 2008; DeKalb et al., 2014). Horn meal was selected as the organic fertilizer, since it is frequently applied as a source of organic N in organic cropping systems (Bunt, 1974; Koller et al., 2004). As a dense material made of hard keratin fibers, horn is a slow-release fertilizer (Paillat et al., 2020) that requires depolymerization of its protein by enzymes due to its physical and chemical recalcitrance (Wang et al., 2016; Zhang et al., 2018).

Compared to MS, we expected OS to have slower microbial processes but higher sensitivity to changes (i.e. fertilization) (Paillat et al., 2020). We also expected that the distribution of enzyme activities would be closely related to nutrient availability. We hypothesized that (1) without fertilization, N- and P-acquiring enzyme activities will be stimulated immediately around roots due to low nutrient availability, especially in OS and high C availability (rhizodeposits), and (2) organic fertilization will stimulate microbial activities (i.e. C-, N- and P-enzyme production and nutrient release) but modify their spatial distribution. More specifically, we expected higher enzyme activities around the fertilization location than in the rhizosphere, especially those of N-acquiring enzymes (LAP and NAG), which are suspected to influence horn-protein depolymerization strongly and microbial turnover. Activities of N and P enzymes may decrease if N and P availability increase due to fertilizer mineralization.

2. Materials and methods

2.1. Experimental design

Rhizoboxes (120 × 120 × 15.8 mm, Fisher Scientific) were used to grow basil in unfertilized and horn-fertilized MS and OS. Basil has a large number of primary, secondary and tertiary roots, and the secondary and tertiary roots are especially sensitive to nutrient availability. MS was sampled from top layer of a cropped loamy soil (0–20 cm) in Reiffenhausen Goettingen (Germany) and dry sieved to 2 mm. It had a bulk density of 0.8 g dw cm^{-3}, a water pH of 6.0 and C and N contents of 10.6 and 1.2 g kg^{-1} dry matter (DM), respectively. The sphagnum peat OS was dry sieved to 10 mm and its water pH was adjusted to 5 using dolomite. It had a bulk density of 0.11 g dw cm^{-3}, and C and N contents of 496.8 and 11.3 g kg^{-1} DM, respectively. Each treatment was performed in triplicate. MS and OS without plants or fertilization (i.e. controls) were also analyzed, with 2 replicates each. Overall, we grew basil in 2 soils (MS or OS) × 2 fertilization levels (with or without) × 3 replicates and used 2 controls (MS or OS) × 2 replicates, for a total of 16 rhizoboxes.

The transparent rhizoboxes were open at the top to allow plants to grow, and one of their short sides could be opened to place membranes or take other measurements (Fig. 1). The rhizoboxes were filled with MS or OS, and their water content was adjusted and maintained at 60 % or 80 % of water holding capacity, respectively, using distilled water. Basil seeds were first germinated on filter paper, then transplanted into seedling trays to straighten into young plants and finally transplanted into the rhizoboxes (i.e. one per rhizobox) 14 days after seedling. For the fertilized treatment, 10 days after transplanting the basil, horn meal (436-136-26 g kg^{-1} DM of C–N–P, respectively) was applied at 50 mg N L^{-1} of soil on the side of the rhizoboxes with the opening, in a single line 3–4 cm long (2.5 cm from the long left side, 4–5 cm from the top and bottom) and lightly covered with MS or OS (Fig. 1A and B). Rhizoboxes

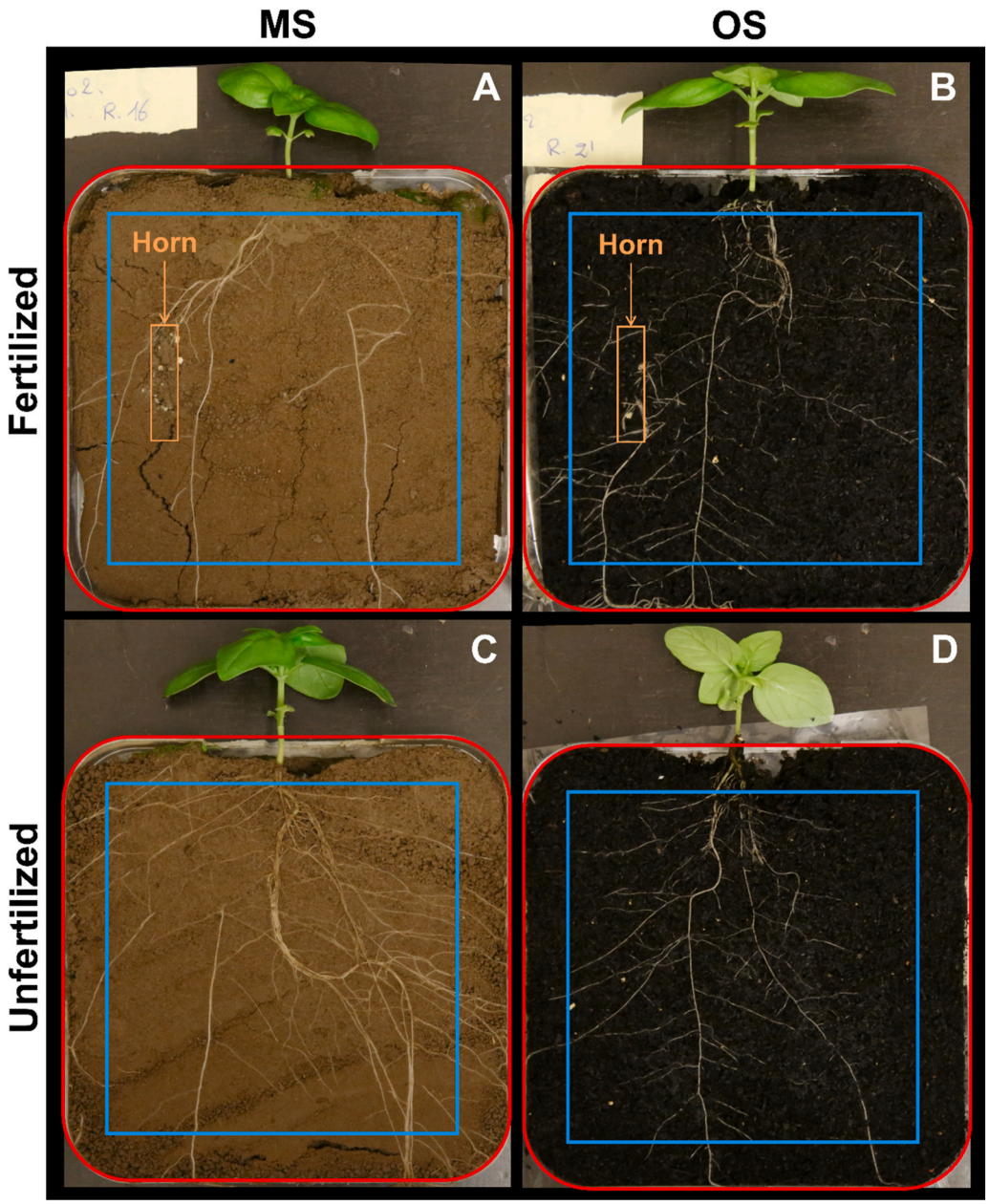

Fig. 1. Photographs of rhizoboxes containing (**A, B**) horn-fertilized or (**C, D**) unfertilized basil grown in (**A, C**) organo-mineral soil (MS) or (**B, D**) organic soil (OS). The red frame indicates the imprint of the enzyme map (zymography) and blue frame the imprint of the nutrient map (diffusive equilibrium in thin films).

were then kept in a climate chamber for 20 days at 24.5 °C with a 16 h:8 h light:dark cycle using LED grow lights (LED K3 XL 450, KIND LED), which provided 500 μmol m^{-2} s^{-1}. During incubation, rhizoboxes were kept tilted at 45° with the side that could open oriented down, which encouraged roots to grow along it (Fig. S1 A).

2.2. Measurement strategy

Twenty days after transplanting the basil, the rhizoboxes were flipped over gently, and the side that could open was opened (Fig. S1 A, B), which allowed zymography and DET to be performed simultaneously (Fig. S1 B). Each sample required 4 successive days to measure (Fig. 2): (1) LAP zymography and NH_4^+ mapping, (2) β-Glu zymography and nitrite and nitrate (NO_2^- and NO_3^-) mapping, (3) acid-P zymography and PO_4^{3-} mapping, and (4) NAG zymography. These combinations of zymography and DET were applied in the same order to all rhizoboxes on 4 successive days (*i.e.* one combination per day for all rhizoboxes).

Briefly, zymography and DET were combined into one device composed of three layers (Fig. S1B). For zymography, a hydrophilic porous membrane (pore size of 0.45 μm, Tao Yuan, China; hereafter, "zymography membrane") saturated with a substrate of a specific enzyme formed the first layer, which was laid directly onto the soil (L1, Fig. S1B; red frame, Fig. 1). Above this membrane, two other layers were taped together to a solid polyvinyl chloride (PVC) plate (slightly smaller than the rhizobox opening) (Fig. S1B) for DET mapping: one protective hydrophilic membrane (~11 × 11 cm; pore size of 0.2 μm, Durapore; hereafter, "DET membrane") (L2, Fig. S1 B) and a probe hydrogel (~10 × 10 cm; hereafter, "DET gel") (L3, Fig. S1 B; blue frame, Fig. 1), which allowed nutrients to be sampled by diffusive equilibrium in water through all three layers (i.e. zymography membrane, DET membrane and DET gel) of the measuring device. Before the experiment, preliminary tests ensured that the reagents used for zymography and DET did not interact. While measuring, the device was covered with aluminum foil to prevent light from influencing the zymography and

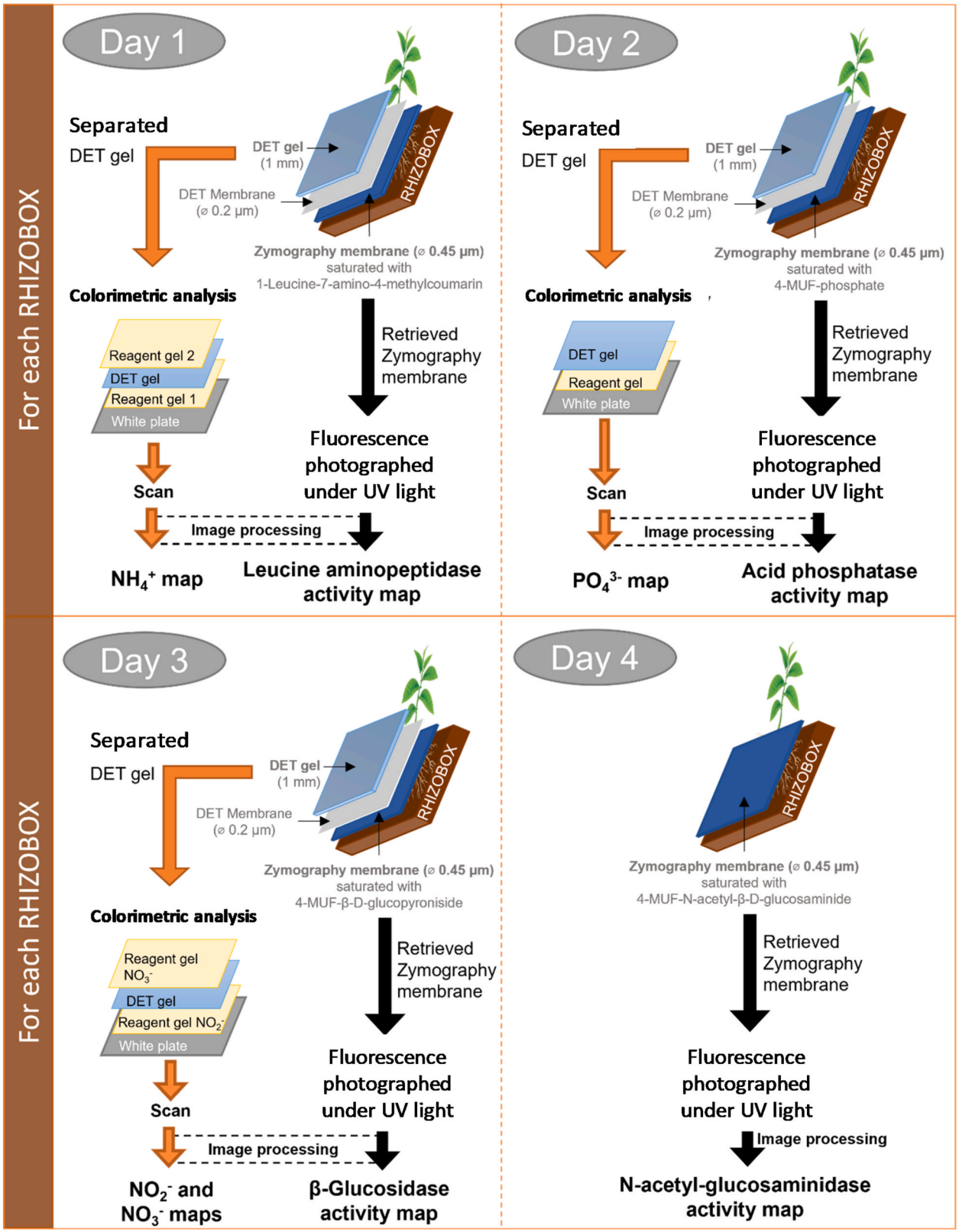

Fig. 2. Measurement procedure on 4 successive days per rhizobox. DET: diffusive equilibrium in thin films, MUF: 4-methylumbelliferone, UV: ultraviolet.

water from evaporating. A weight was placed on the PVC plate to increase contact between the three layers and the sample during 2 h of incubation, after which the weight and aluminum foil were removed, and the device was dismantled: the zymography membrane and DET device were carefully separated and then processed separately using ultraviolet (UV) fluorescence and colorimetric analysis, respectively (Fig. 2).

Immediately after measuring NAG activity on day 4, roots were gently removed from the MS or OS and washed to remove all particles. The roots, stem and leaves of each plant were washed, and the leaves

were scanned using WinRhizo software (Arsenault et al., 1995) to estimate the total leaf area per plant (cm^2). The roots, stem and leaves were oven dried at 60 °C for 48 h and then weighed to measure shoot (stem + leaves) and root biomass. The root:shoot ratio was calculated by dividing root biomass by shoot biomass.

2.3. Measuring enzyme activity using zymography

The zymography membranes were saturated with fluorescent dye [4-methylumbelliferone (MUF) or 7-amino-4-methylcoumarin (AMC)] conjugated with enzyme substrates (Razavi et al., 2019): 4-MUF-β-D-glucopyranoside, 4-MUF-N-acetyl-β-D-glucosaminide, L-leucine-AMC and 4-MUF-phosphate to determine β-glu, NAG, LAP and acid-P activities, respectively (Fig. 2). Enzyme substrate solutions were prepared at 1 mM in a buffer: MES (pH 6.5, 0.1 M) for MUF substrates (β-Glu, NAG and acid-P) and TRIZMA (pH 7.2, 0.05 M) for the AMC substrate (LAP).

Since the zymography membrane had been in direct contact with the soil, it was cleaned with a small brush before being laid on a black plate and photographed (Canon EOS 6D camera with a Canon EF 24–105 lens) under UV light (Supratec 18 W/73 UV-A lamp, OSRAM) (Fig. 2). To determine calibration curves, small pieces of another zymography membrane (4 cm^2, ⌀ 0.45 μm, Tao Yuan, China) were saturated with standard solutions of MUF or AMC (from 0 to 1 mM) and processed as described for the samples.

2.4. Mapping nutrients using the method of diffusive equilibrium in thin films

DET is based on colorimetric analyses that estimate nutrient concentrations: the nitroprusside method (Keeney and Nelson, 1982) for NH_4^+, the molybdenum blue method (Murphy and Riley, 1962) for PO_4^{3-}, the Griess method (Moorcroft et al., 2001) for NO_2^-, and the Griess method combined with the reduction of NO_3^- into NO_2^- using vanadium chloride for $NO_2^- + NO_3^-$ (Miranda et al., 2001). These methods were adapted for 2D imaging; thus, the colorimetric reactions occurred in hydrogels according to Metzger et al. (2019) for NH_4^+ imaging, Metzger et al. (2016) for NO_2^- and $NO_2^- + NO_3^-$ imaging, and Cesbron et al. (2014) for PO_4^{3-} imaging.

Two types of hydrogels were used: the DET gels to sample nutrients and "reagent gels", which contain 95–98 % water and are saturated with polyacrylamide or agarose, to react in the colorimetric analyses (Fig. 2). We used polyacrylamide gels (1 mm thick) prepared according to Jézéquel et al. (2007) to measure $NO_2^- + NO_3^-$ and PO_4^{3-} concentrations and agarose gels prepared according to Metzger et al. (2019) to measure NH_4^+ concentration, since the amide groups in polyacrylamide may interact with reagents of NH_4^+ analyses (Metzger et al., 2019). Until being used for measurements, polyacrylamide gels were stored in distilled water at room temperature, while agarose gels were stored in a refrigerator (4 °C).

To achieve the colorimetric reaction, the DET gel was either placed in contact with one reagent gel (*i.e.* PO_4^{3-} and NO_2^-) or sandwiched between two reagent gels (*i.e.* NH_4^+ and $NO_2^- + NO_3^-$) on a white PVC support plate (Fig. 2). Reagent gels were prepared and then assembled with the associated DET gel After each colorimetric analysis, the gel assembly was scanned, and the image obtained was processed to determine nutrient availability.

Standard solutions were prepared from NO_3NH_4, $NaNO_2$, $NaNO_3$ and K_2HPO_4 salts to determine NH_4^+, NO_2^-, NO_3^- and PO_4^{3-} calibration curves, respectively, at concentrations that ranged from 0 to 540, 135, 180 or 720 μM, respectively. A hydrogel, – DET gel (polyacrylamide or agarose, depending on the ion) – was placed between two polycarbonate plates pressed together using clamps. The top plate had wells in which 3.5 mL of standard solution was poured onto the gel, covered by caps and left for at least 1 h to equilibrate. The same steps of colorimetric analysis as for the DET gels were then performed.

2.5. Image processing

Images (*i.e.* zymograms and DET scans) were processed using ImageJ Fiji software (Schindelin et al., 2012). Zymograms were converted into 8-bit grayscale images, and the gray values obtained were then min-max normalized from 0 (black) to 255 (white) (Sane and Agrawal, 2017). These images were then converted into enzyme activities using the normalized calibration curves with set maxima to obtain a concentration scale for all images using ImageJ Fiji. Thus, data could be considered as semi-quantitative. DET scans were stripped of their edges and broken down into primary-color intensities of red, green and blue channels, which were converted into 8-bit grayscale images. The most sensitive channel was selected for each ion: red for NH_4^+ and PO_4^{3-} and green for NO_2^- and NO_3^- (Cesbron et al., 2014; Metzger et al., 2016, 2019). As before, the gray values were then normalized from 0 (black) and 255 (white). Results of gray-scaled matrices were then converted into concentrations using the calibration curves for all images using a modified procedure of Thibault de Chanvalon et al. (2015) in R software (v. 3.5.1) (R Core Team, 2020).

2.6. Data processing

To determine the change in enzyme activity, we considered two methods that required defining a threshold (Razavi et al., 2019; Bilyera et al., 2020) at which an increase in enzyme activity (compared to a baseline) was considered significant (i.e. "hotspot"). Hotspots are thus small volumes of soil in a rhizobox that have more rapid processes than the rest of the area sampled (Kuzyakov and Blagodatskaya, 2015). We selected the method that calculated hotspots as a percentage of the highest enzyme activity in a zymogram (Razavi et al., 2019), which was more suitable for the study's contrasting soil conditions. For LAP activity, we set the threshold for hotspots at 10 % of the highest activity to compare MS and OS zymograms. We attributed enzyme activities to roots or fertilization in each zymogram and then estimated their relative contributions to total hotspot activity as their ratio (hereafter, "root: fertilization activity ratio").

For β-glu, NAG, and acid-P activities, the thresholding methods could not be used due to the lack of contrast in their distributions. Thus, to compare their activities in the rhizosphere to those in the bulk soil, we calculated one mean activity for each of these areas per rhizobox by measuring at least 5 random squares of 10 × 10 pixels of distinguishable roots or 150 × 150 pixels of bulk soil in each zymogram (Spohn et al., 2015).

2.7. Statistical analyses

R software (v. 3.5.1) was used for all statistical analyses. Differences between fertilized and unfertilized soil and, when determined, between enzyme-activity locations (bulk soil, rhizosphere, fertilization location) were analyzed using two-way analysis of variance (ANOVA) followed by *post-hoc* Tukey's HSD tests. Differences were considered significant at $p < 0.05$. The normality of the residuals and homoscedasticity were tested previously using the Shapiro-Wilk and Bartlett's tests, respectively. When these assumptions were not met, we used the non-parametric Kruskal-Wallis and Wilcoxon-Mann-Whitney tests, respectively.

3. Results

3.1. Two-dimensional nutrient distribution

NH_4^+ concentration in MS reached gel saturation (>1000 μM) in the center of the fertilization location, which decreased to the NH_4^+ a concentration in the bulk soil similar to those in the controls (74 μM) (Fig. 3A). The highest NH_4^+ concentration extended laterally for 1.5 cm from the center of the fertilization location (1.5–3.0 cm, Fig. 3B), while a concentration of 200 μM extended as far as 6 cm from the left side of the

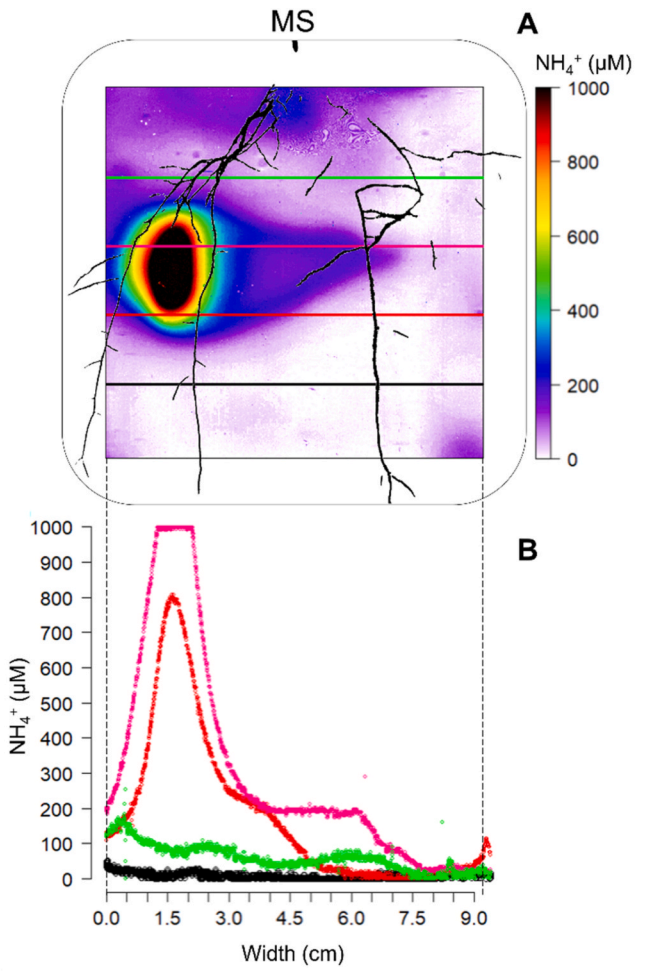

Fig. 3. Example of NH_4^+ concentration (μM) in fertilized mineral soil (MS) with plants in (**A**) two-dimensional images and (**B**) transects of its distribution (n = 3, semi-quantitative). The colors of the transects in **A** correspond to those of the curves in **B**.

rhizobox (magenta line, Fig. 3B). In OS, NH_4^+ concentration was not influenced by fertilization or roots and did not exceed 200 μM (data not shown).

Fertilization increased NO_2^- concentration in both MS and OS ($p < 0.05$). NO_2^- concentration was highest in the center of the fertilization location (Fig. 4A–C) in both MS and OS and diffused further in MS (Fig. 4B–D).

NO_3^- concentration reached gel saturation (220 μM) in both controls (data not shown). In planted MS, NO_3^- concentration reached gel saturation in both unfertilized and fertilized treatments but sometimes remained below saturation in the center of the rhizobox. In planted OS, NO_3^- concentration was significantly lower than that in the control due to plant uptake ($p < 0.001$). Fertilization increased NO_3^- concentration at the fertilization location, which reached gel saturation in its center (Fig. 5A and B).

PO_4^{3-} concentration was influenced only by the plants in OS, being lower in planted OS (unfertilized or fertilized) than in the control ($p < 0.001$), which had the highest concentrations (Fig. 6A). In the planted treatments, PO_4^{3-} concentrations were highest in the areas without roots at the bottom and edges of the rhizoboxes (Figs. 6B and 4C). PO_4^{3-} concentration in MS was low (<0.1 μM) in all treatments (control, unfertilized or fertilized plants) and had no clear spatial distribution (data not shown).

3.2. Two-dimensional enzyme activity distribution

3.2.1. Leucine aminopeptidase activity

Plants and fertilization changed the spatial distribution of LAP ($p < 0.01$) in MS and OS (Figs. 7 and 8). In the controls, MS had higher LAP activity and spatial variability than OS did (Fig. S2). In unfertilized MS, LAP activity was larger around roots and root tips than in the bulk soil ($p < 0.01$, Fig. 8A and B). In fertilized MS, LAP activity around roots was similar to that in the bulk soil (Fig. 8C and D). LAP activity around the fertilization location reached saturation of the method used (9 pmol mm^{-2} h^{-1}) and thus exceeded that around roots. Fertilization and root locations influenced LAP activity in planted OS ($p < 0.05$). LAP activity was larger around roots (Fig. 7A), especially around root tips, than in the unfertilized bulk soil (Fig. 7B–D). Fertilization further increased LAP activity around roots and root tips (Fig. 7C and D) and the fertilization location (Fig. 7C–E).

3.2.2. 1.4-β-glucosidase, N-acetyl-glucosaminidase and acid-phosphatase activities

Mean β-Glu activity was influenced by the soil type (MS *vs.* OS) and location (bulk soil *vs.* rhizosphere) in the rhizobox (soil type × location interaction, $p < 0.01$), but no fertilization effect was observed. Mean β-Glu activity was higher in the bulk soil than in the rhizosphere (92.1 and 45.2 pmol mm^{-2} h^{-1}, respectively) in MS, but not in OS. Mean β-Glu activity in the bulk soil was higher in MS than in OS (Fig. 9A–D). In the controls, mean β-Glu activity was higher in MS than in OS (51 ± 5.9 and 26.2 ± 1.3 pmol mm^{-2} h^{-1}, respectively; Fig. 9A–D).

Mean NAG activity was influenced by the soil type and location (bulk soil *vs.* rhizosphere) in the rhizobox (soil type × location interaction, $p < 0.05$) but not by fertilization. Mean NAG activity of bulk soil was higher in MS than in OS (Fig. 9B–E). In both MS and OS, mean NAG activity was higher in the bulk soil than in the rhizosphere (Fig. 9E–B). See Fig. S3 for examples of NAG zymograms. In the controls, mean NAG activity was higher in MS than in OS (46.7 and 24.5 pmol mm^{-2} h^{-1}, respectively; Fig. 9B–E).

Mean acid-P activity was influenced mainly by its location in the rhizobox (location effect, $p < 0.001$) and to a lesser extent by the soil type (soil effect, $p < 0.05$). In MS and OS, mean acid-P activity was the highest near roots (21.7 pmol mm^{-2} h^{-1}). In the controls, mean acid-P activity was similar in MS and OS (14.3 and 16.7 pmol mm^{-2} h^{-1}, respectively; Fig. 9C–F).

3.3. Effects of fertilization and soil type on plant growth parameters

The soil type × fertilization interaction had a significant effect on plant root biomass ($p < 0.05$), stem biomass ($p < 0.01$), leaf biomass ($p < 0.001$) and leaf area ($p < 0.01$). The root:shoot ratio was lower with fertilization (fertilization effect, $p < 0.05$). Fertilization halved shoot biomass in MS but doubled stem and leaf biomasses (Fig. 10A) and leaf area (Fig. 10B) in OS.

4. Discussion

4.1. Distributions of enzyme activities and nutrients in the rhizosphere

Nutrient availability depends on soil properties (e.g. pH, water content, organic matter content, texture, temperature, microbial activity), which influence mineralization, dissolution, desorption and diffusion processes (Comerford, 2005). In this experiment, temperature and water content were set to optimize microbial activity (Voroney and Heck, 2015) and adapted for basil growth (Putievsky, 1983). The pH was also set to optimize N and P availabilities at the beginning of experiment (Caron et al., 2003; Guber and Kravchenko, 2024).

While zymography strongly reflects the enzyme activity around roots, DET imaging increases diffusion of small molecules into the soil solution. Zymography and DET imaging are based on diffusion in the

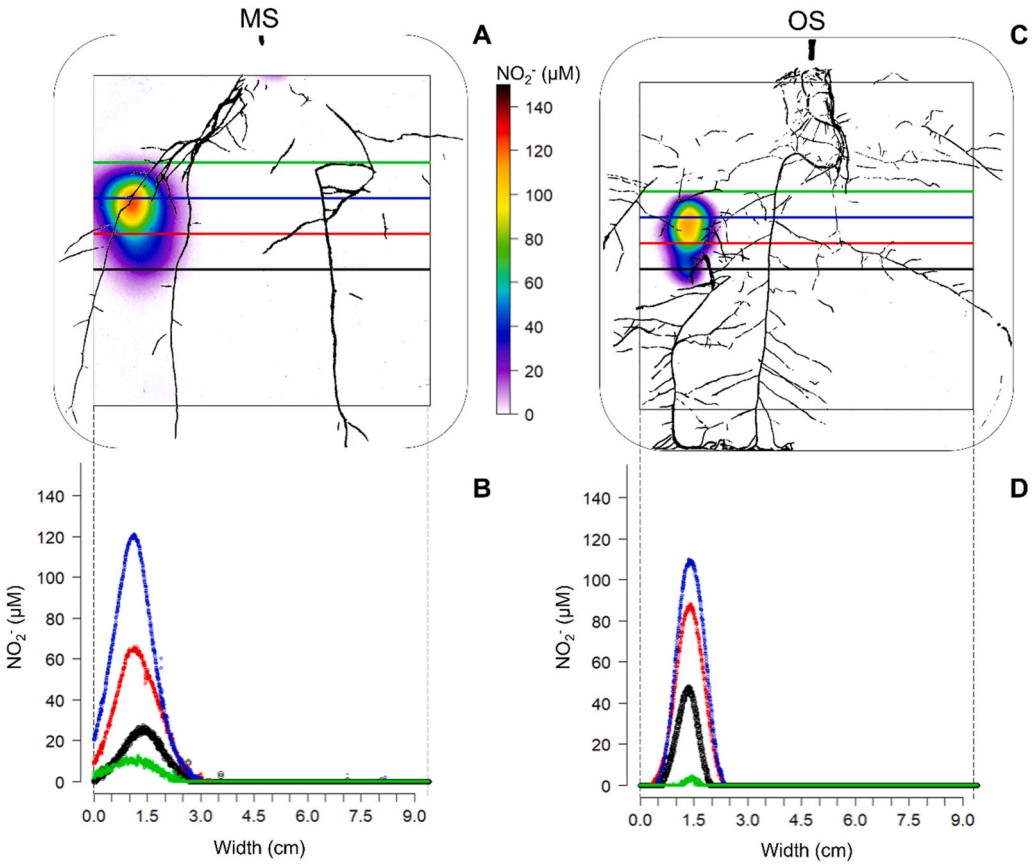

Fig. 4. Examples of NO_2^- concentration (μM) in the fertilized treatments with plants in (**A, B**) mineral soil (MS) or (**C, D**) organic soil (OS) in (**A, C**) two-dimensional images and (**B, D**) transects of its distribution (n = 3, semi-quantitative). The colors of the transects in **A** and **C** correspond to those of the curves in **B** and **D**, respectively.

pore water of soil samples. Their results depend greatly on the degree of contact between the sample and the measuring device (Guber et al., 2018; Razavi et al., 2019; Loginova and Bilyera, 2025), which consisted of two membrane layers and a hydrogel in the present study. We combined, for the first time, mapping of distributions of NH_4^+ concentration and LAP activity, $NO_2^- + NO_3^-$ concentrations and β-Glu activity, and PO_4^{3-} concentration and acid-P activity in two soil types, and measured that of NAG activity separately. Nutrient mineralization is caused by stepwise multi-enzyme processes (Nannipieri et al., 2018). In agreement with results of Paillat et al. (2020), enzyme activities in the present study were not strongly correlated with nutrient concentration, which reflects the complexity of biogeochemical cycling. Direct relations between enzyme activity and nutrient concentration were observed only for mineral N, and were illustrated more accurately in OS due to its slower processes.

4.1.1. *Fertilizer effects on enzyme and nutrient distributions*

Microbes first increased the concentration of mineral N in the soil as NH_4^+ at the organic fertilization location by mineralizing the organic fertilizer (Fig. 3), which paralleled LAP activity (Fig. 8C–F), which is involved in protein hydrolysis (Plante et al., 2015). In MS, LAP activity and NH_4^+ concentration were highest at the fertilizer location, and they extended up to 1.5 cm from its center into the bulk soil. Fertilizer mineralization supported strong nitrification, which generated high NO_2^- and NO_3^- concentrations at the fertilization location (Figs. 4 and 5). The saturated NO_3^- concentration in DET gel also suggested that nitrification was not limiting but made it difficult to assess the fertilizer effect in MS.

In OS, the fertilization effect on LAP activity varied more, and thus its magnitude was difficult to assess (Fig. 7F). NH_4^+ concentration was zero outside of the fertilizer location, likely because it was taken up immediately by nitrifiers. Nitrification may be slower in OS than in MS, as suggested by the lower NO_2^- and NO_3^- concentrations, especially at the fertilizer location (Figs. 4 and 5).

To our knowledge, this study is the first to have mapped enzyme activities in highly fertilized soils. Despite the preliminary tests, this study identified room for improvement to obtain more sensitive and accurate results. In particular, both MS and OS had saturated NO_3^- concentrations in the control (*i.e.* > 220 μM), but NO_3^- is usually observed in soil solutions at mM concentrations (Richardson et al., 2009) (i.e. 10 times as high as those measured in the study). In OS, the rhizosphere contained little NO_3^-, while in MS, NO_3^- concentration was only slightly lower in the center of rhizoboxes, which indicates that the method used may be too sensitive in matrices in which nitrification is strong, especially since NO_3^- diffuses rapidly in pore water. Methodological improvements are necessary to measure NO_3^- concentrations in the ranges observed in soil. Using a hyperspectral camera instead of a traditional scanner may increase data resolution and thus the range of concentrations covered (Metzger et al., 2016).

4.1.2. *Root effects on enzyme and nutrient distributions*

Root presence influenced nutrient distributions little but LAP activity strongly, the latter due directly to LAP exudation by roots or indirectly to stimulation of microbial activity by rhizodeposition (Richardson et al., 2009; Razavi et al., 2016; Song et al., 2022). The lack of a relation between root presence and nutrient distributions likely indicates that the method used cannot accurately capture this effect with young plants and that rates may be too slow. Conversely, it is possible that mobile nutrients (depending on their type) could not be captured by measuring them only after 20 days.

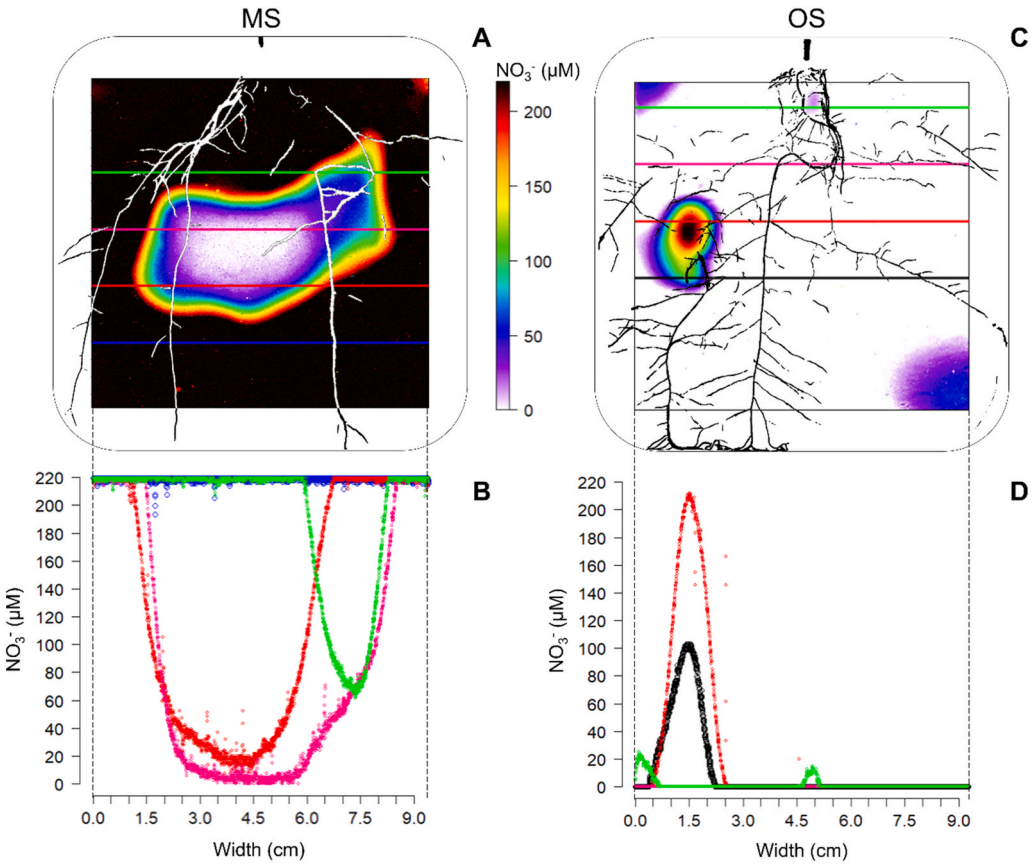

Fig. 5. Examples of NO_3^- concentration (μM) in the fertilized treatment with plants in (**A, B**) mineral soil (MS) or (**C, D**) organic soil (OS) in (**A, C**) two-dimensional images and (**B, D**) transects of its distribution (n = 3, semi-quantitative). The colors of the transects in **A** and **C** correspond to those of the curves in **B** and **D**, respectively. No hotspot of NO_3^- concentration caused by fertilization could be identified in MS; thus, only plant uptake of NO_3^- could be assessed. The hotspot in OS begins where the red and black curves begin to increase, since NO_3^- was not detected outside of the hotspot.

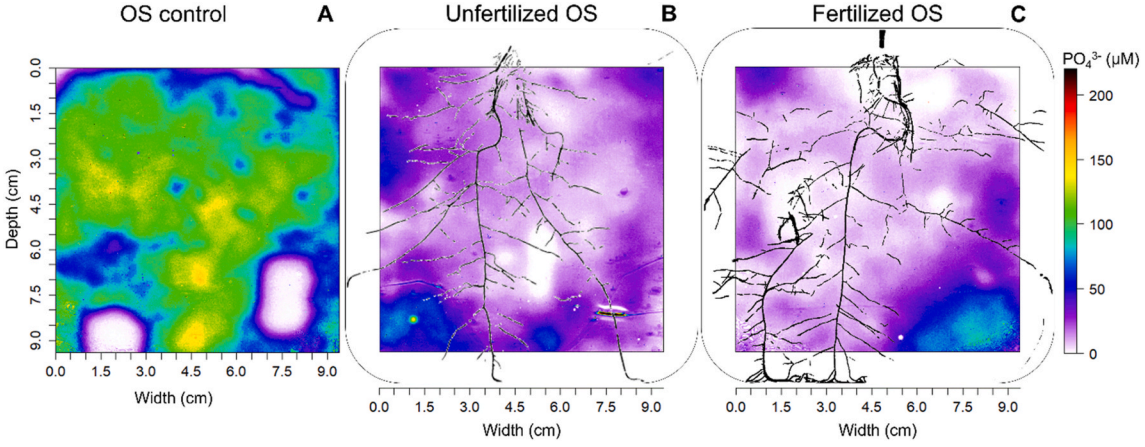

Fig. 6. Distribution of PO_4^{3-} concentration (μM) in the organic soil (OS) (**A**) control (without plants or fertilization), (**B**) unfertilized treatment with plants and (**C**) fertilized treatment with plants.

LAP activity was high in OS (50 % of the OS area had higher LAP activity than the bulk OS control did) (Fig. S2). LAP was especially sensitive to root presence in OS (Figs. 7 and 8) and responded strongly to fertilization, extending to the bulk soil. The 1–2 mm extent of the rhizosphere as measured by LAP activity was consistent with that in previous studies (Marschner et al., 2012; Razavi et al., 2016; Ren et al., 2021). Exudation around root tips explained this high LAP activity, in agreement with many theories for non-leguminous plants (Hinsinger, 1998; Pausch and Kuzyakov, 2011; Razavi et al., 2016).

At the same time, NO_3^- concentration in both unfertilized and fertilized soils with plants decreased greatly compared to that in the controls (without fertilizer or plant), which indicated a strong rhizosphere effect caused by root uptake and/or an increase in microbial activities. OS also had a low NH_4^+ concentration; thus, root exudates caused strong microbial responses in the OS rhizosphere that were not observed in the control OS (without plants). These results confirm the nutrient limitation of microbes in OS: new organic compounds supplied by fertilization and rhizodeposits would stimulate microbial activities

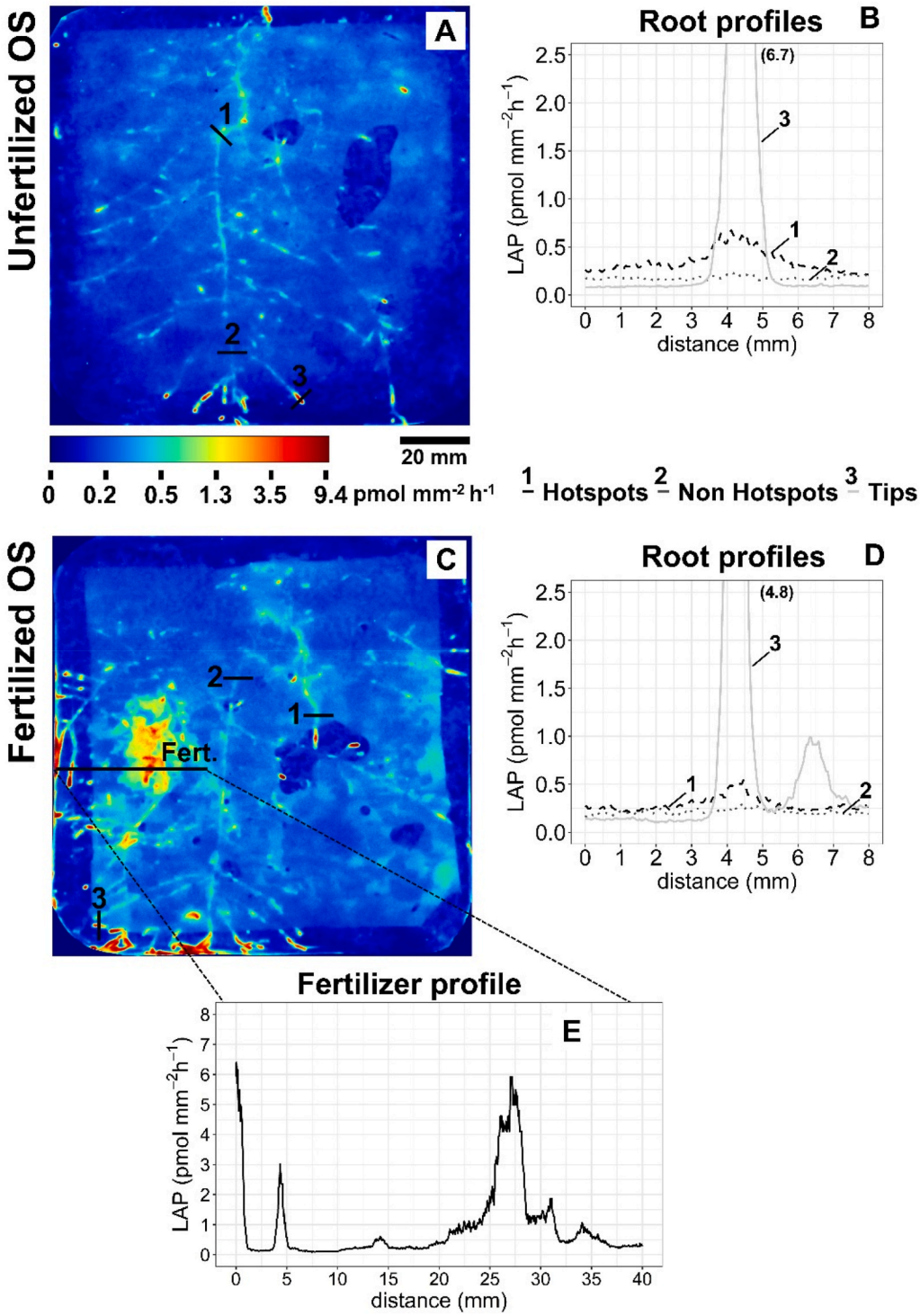

Fig. 7. Distribution of leucine aminopeptidase (LAP) activity (pmol mm^{-2} h^{-1}, semi-quantitative) in (**A**) unfertilized and (**C**) fertilized organic soil (OS) with plants, with black bars indicating the locations of activity profiles (**B** and **D**, respectively) (1) in hotspots, (2) in non-hotspots and (3) around root tips "Fert." in **C** identifies the location of (**E**) the fertilizer profile.

strongly. The low N concentrations that contrasted with high LAP activity suggested high nutrient limitations on microbes, which leads to competition for N in the rhizosphere (Kuzyakov and Xu, 2013). In MS, determining the degree to which roots contributed to LAP-activity hotspots was more difficult, since some of the bulk soil also had hotspots (Figs. 7 and 8) and sometimes had higher LAP activity than the roots did (Fig. 8E), especially in fertilized MS. In addition, since nutrients (especially N) were available for root uptake, plants may have invested less in rhizodeposits, which explains why, unlike in OS, root tips were less identifiable as hotspots in MS. A rhizosphere effect on NO_3^- distribution was indeed suspected, since NO_3^- concentration decreased in the center of the rhizobox.

Since β-Glu is a hydrolytic enzyme involved in cellulose degradation, N availability to microbes stimulates β-Glu activity (Allison and Vitousek, 2005; Jian et al., 2016). However, the relation between NH_4^+ concentration and β-Glu activity is difficult to assess, since NH_4^+ is often

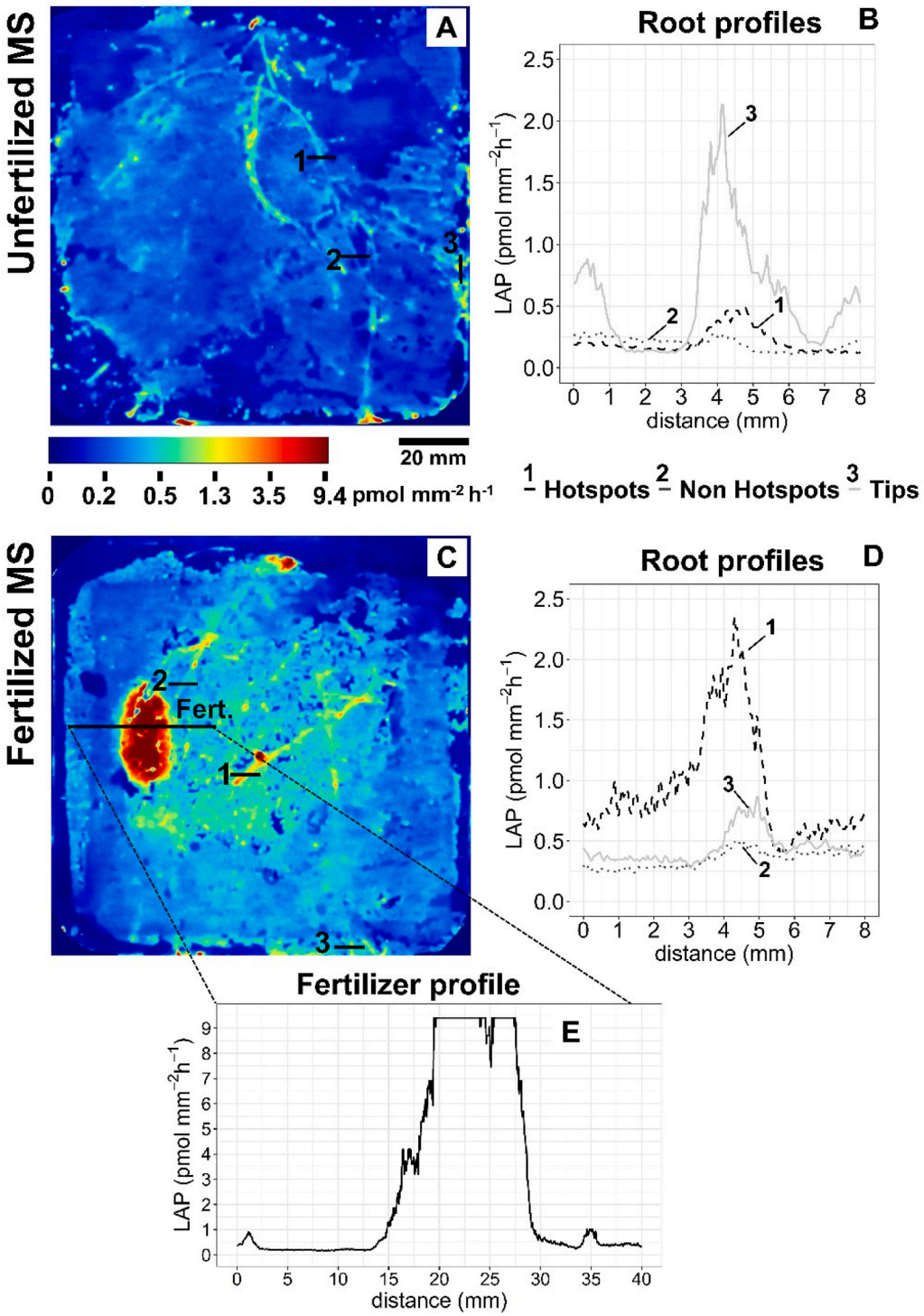

Fig. 8. Distribution of leucine aminopeptidase (LAP) activity (pmol mm^{-2} h^{-1}, semi-quantitative; color scale on the bottom) in (**A**) unfertilized and (**C**) fertilized mineral soil (MS) with plants, with black bars indicating the locations of activity profiles (**B** and **D**, respectively) (1) in hotspots, (2) in non-hotspots and (3) around root tips "Fert." in **C** identifies the location of (**E**) the fertilizer profile.

rapidly immobilized in microbial biomass. N availability to microbes controls NO_3^- release by nitrification, and thus complete mineralization could be considered. The spatial distribution of NO_3^- concentration and β-Glu activity was less clear than expected in both MS and OS soils (Fig. S4). In OS, whether fertilized or not, β-Glu activity was limited by NH_4^+, as reflected by the low NO_3^- concentration (Fig. 5A). In MS, two replicates (one fertilized, one unfertilized) had especially high β-Glu activity and the largest decrease in NO_3^- concentration in the center of the rhizobox (Fig. S4). In other areas we suspect a lack of contact between the zymography membrane and the soil that would explain a lack of enzymatic activity (upper right zone, Fig. S4). In one of these rhizoboxes, NAG activity, involved in fungal biomass turnover (Leveau and Preston, 2008) due to being involved in chitin hydrolysis, and LAP activity were also higher in the center (data not shown). These high NAG and LAP activities and low NO_3^- concentrations in the center of the rhizoboxes were not strongly related to the root system being less dense

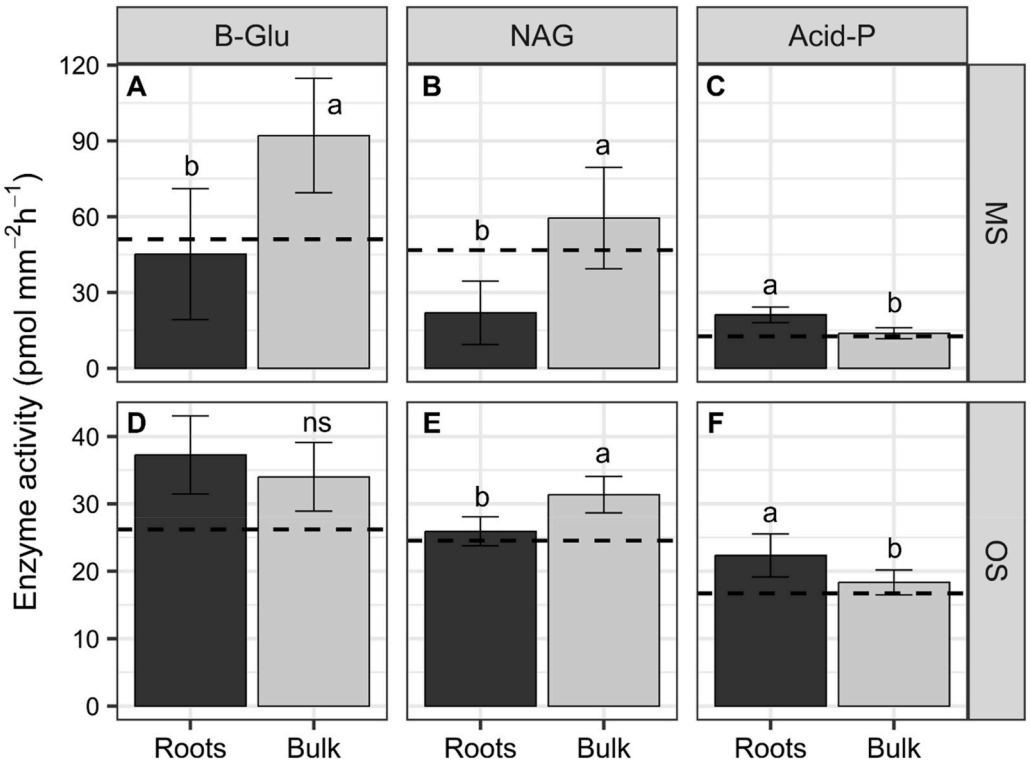

Fig. 9. Mean (±1 standard deviation) activities of 1.4-β-glucosidase (β-Glu), N-acetyl-glucosaminidase (NAG) and acid-phosphatase (Acid-P) (pmol mm^{-2} h^{-1}, semi-quantitative) in the rhizosphere and bulk soil of in planted mineral soil (MS) and organic soil (OS) (n = 6). Dashed lines represented background activities in the controls (without plants or fertilization). Different letters indicate significant differences between rhizosphere and bulk soil locations and "ns" indicates non-significant differences between rhizosphere and bulk soil locations.

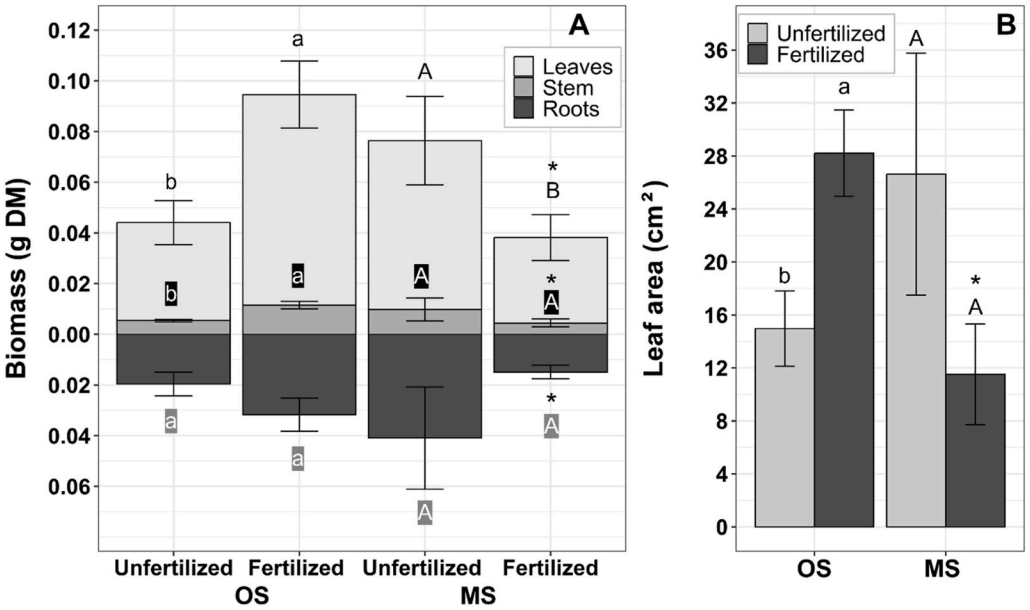

Fig. 10. Mean (±1 standard deviation) (**A**) root, stem and leaf biomasses (g dry matter per plant) and (**B**) leaf area (cm^2 per plant) of plants grown in unfertilized or horn-fertilized organic soil (OS) or mineral soil (MS) 20 days after transplantation (n = 3). Different lower-case letters indicate significant differences ($p < 0.05$, Student's *t*-test) between unfertilized and fertilized treatments in OS (and upper-case letters for MS respectively) (**A,B**), with respectively black letters for leaves biomass, white letters on black background for stem biomass and white letters on gray background for root biomass (**A**). Asterisks indicate significant ($p < 0.05$, Student's *t*-test) differences between soils (OS vs. MS) for a given treatment (unfertilized or fertilized) (**A,B**).

there. For example, non-visible roots (under the soil-rhizobox interface) could have stimulated active soil microbes with their exudates, which in turn increased microbial nutrient demand and enzyme expression (Liu et al., 2017) and induced competition between plants and microbes for N in the rhizosphere (Kuzyakov and Xu, 2013).

The weak effects of the rhizosphere on β-Glu, NAG and acid-P activities was not expected (Fig. 9), since many studies have observed strong and direct effects of roots on them (Spohn and Kuzyakov, 2014;

Ge et al., 2017; Ma et al., 2018). However, roots sometimes have more variable effects on acid-P activity (Ge et al., 2017; Kuzyakov and Razavi, 2019), especially when the detritusphere is involved (Ma et al., 2017). The weak response of these enzyme activities could indicate non-limiting nutrient conditions or the presence of enzymes stabilized on the soil matrix that were not related to more recent microbial activities. These activities would no longer have been regulated by viable microbes, since they would have stabilized and accumulated on the matrix while remaining catalytic (Nannipieri et al., 2018). This explanation agrees with results of Knight and Dick (2004), who observed in three soils that 34–75 % of β-Glu activity came from stabilized enzymes. The abiotic enzymes Acid-P, β-Glu and NAG can be inherited from source soils. This is likely to be true for acid-P in OS, as observed by Paillat et al. (2020).

4.2. Plant-growth parameters and relations with enzyme and nutrient distributions

In OS, plant growth and leaf area (Fig. 10) increased under organic fertilization that created locally higher NH_4^+ and NO_3^- concentrations (Figs. 3 and 5) and LAP activity (Figs. 7 and 8). Larger plants and leaves transpire more, which causes plants to have larger water flows and nutrient uptake (Comerford, 2005; Matimati et al., 2014). Thus, we expected that the low N and P concentrations in unfertilized OS (Figs. 5 and 6) would not be able to sustain these processes. However, plant growth and nutrition soon decreased (i.e. leaves turned yellowish) in the fertilized OS, which suggested that the plants soon became nutrient-limited (and remained so 6 and 7 weeks after transplantation; Fig. S5 and S6) due to high competition with microbes, which took up all of the added nutrients. In MS, fertilization stimulated LAP activity (Figs. 3 and 8), which increased the amount of N released (Figs. 4 and 5) but decreased plant growth, since the N concentration likely reached a level toxic for young plants (Bernstein et al., 2010; Attia et al., 2011; Bekhradi et al., 2015). This phase was temporary, and plants soon made up for the slower growth. Indeed, plants in fertilized MS produced the most biomass 6 and 7 weeks after transplantation (Fig. S5 and S6), and likely had the highest N content in leaves over the long term (data not shown). Thus, the N-toxicity threshold might have been increased by the increasing nutrient demand for plant growth. In addition, high microbial activities in certain MS replicates (Fig. S4) suggested an increase in microbial growth and thus microbial nutrient demand and enzyme activities (Liu et al., 2017). This may cause temporary competition for nutrients between roots and microbes, but root-microbe interactions favor plants over the long term (Kuzyakov and Xu, 2013). In OS, however, the increase in nutrient demand during plant growth increased this competition, and the fertilization could not supply both plants and microbes (Fig. S5 and S6). The higher NO_3^- concentration in fertilized OS, in which plants seemed to be N-limited, stimulated root elongation, while accumulation of NO_3^- in shoots decreased root growth in MS (Mantelin and Touraine, 2004), which led to a lower root:shoot ratio in fertilized MS than in unfertilized MS (Fig. 10).

The relationship between available P and acid-P was not sharp (Fig. S8). The low P concentration in the soil solution of MS did not necessarily mean little P bioavailable for plants, whose leaves showed no signs of P deficiency (Fig. S5 and S6). P concentration and acid-P activity sometimes increased slightly in the MS rhizosphere (Fig. S7), perhaps due to (1) local rhizosphere acidification (Hinsinger, 1998) that caused desorption or (2) slightly higher acid-P activity in the rhizosphere (Fig. 8). Consequently, P mineralized from fertilizers can be taken up by roots and microbes and/or adsorbed onto the soil matrix. In OS soil, higher acid-P did not mean higher available P and sometimes the contrary (Fig. S8) possibly illustrating higher absorption (taken up by roots and microbes) than P release from acid-P activity. The contribution of hydrolyzed P added with MUF-P to PO_4^{3-} concentration could be considered, especially in MS (Hummel et al., 2021). However, P concentrations in our probes were 6 times lower than this pioneering work suggesting lower overestimation.

5. Conclusions

This study observed contrasting rhizosphere functioning in relation to nutrient availability in mineral (MS) and organic (OS) soils. Nutrient limitation of plants and microbes induced strong competition for nutrients, and thus available N and P decreased greatly, which limited plant growth. In MS, fertilization was not needed to maintain plant or microbial growth. Fertilization did not change enzyme activities in the rhizosphere or bulk soil. However, the high mineralization (high LAP activity and N release at the fertilization location) and nitrification rates in MS decreased plant growth, likely due to high nutrient concentrations in the small volume of the rhizoboxes (*i.e.* temporary toxicity).

Zymography and DET mapping, combined here for the first time in this study, revealed the spatial distribution of these respective processes involved in the rhizosphere and the fertilization location. These mapping methods are particularly relevant for studying the influence of local organic fertilization on rhizosphere functioning in OS. Indeed, OS responded the most since it is a stressful nutrient habitat for microbes and plants, which made it easier to determine the relative contributions of roots, root tips and fertilizer to microbial hotspots in relation to nutrient availability. In this way, this study developed a novel tool for advancing many types of rhizosphere-related research in agriculture and horticulture.

CRediT authorship contribution statement

L. Paillat: Writing – review & editing, Writing – original draft, Visualization, Validation, Resources, Methodology, Investigation, Formal analysis, Data curation, Conceptualization. **P. Cannavo:** Writing – review & editing, Writing – original draft, Validation, Supervision, Resources, Project administration, Methodology, Funding acquisition, Data curation, Conceptualization. **A. Mouret:** Writing – review & editing, Methodology. **E. Metzger:** Writing – review & editing, Methodology. **L. Huché-Thélier:** Writing – review & editing, Validation, Supervision, Methodology, Funding acquisition, Conceptualization. **F. Barraud:** Writing – original draft. **A.S. Azimi:** Writing – original draft, Investigation. **J. Cardenas:** Investigation, Formal analysis. **C. Banfield:** Writing – original draft, Resources, Project administration. **Y. Kuzyakov:** Writing – original draft, Supervision, Methodology. **M. Dippold:** Writing – original draft, Supervision, Resources, Project administration, Methodology. **R. Guénon:** Writing – review & editing, Writing – original draft, Validation, Supervision, Methodology, Investigation, Funding acquisition, Conceptualization.

Funding

This research was funded by the Premier Tech GHA company and the French National Association of Research and Technology (Association Nationale de la Recherche et de la Technologie) (CIFRE, 2017/0752). This study also received two grants from The Ecology, Geosciences, Agronomy & Food (EGAAL) Doctoral School and from Credit Agricole Ile-de-France Mécénat in collaboration with the French Academy of Agriculture.

Declaration of competing interest

The authors declare the following financial interests/personal relationships which may be considered as potential competing interests: Patrice Cannavo reports financial support was provided by Premier Tech Ltd. If there are other authors, they declare that they have no known competing financial interests or personal relationships that could have appeared to influence the work reported in this paper.

Acknowledgments

We thank Nisha Bhattarai (BGC department, Göttingen University, Germany) for its help during the experiment. We thank the following people for their help during methodological development and preliminary tests: Constance Choquel (LPG UMR 6112, Angers University, France), Bahar Razavi (Kiel University, Germany) and, from the BGC department of Göttingen University, Nataliya Bilyera and Liang Wei. We also thank Keith Edwards (Ecosystem Biology department of South Bohemia University, České Budějovice, Czech Republic) for helping with data analysis and WinRhizo® analysis, respectively.

Appendix A. Supplementary data

Supplementary data to this article can be found online at https://doi.org/10.1016/j.soilbio.2025.110039.

References

Allison, S.D., Vitousek, P.M., 2005. Responses of extracellular enzymes to simple and complex nutrient inputs. Soil Biology and Biochemistry 37, 937–944.
Arsenault, J.-L., Poulcur, S., Messier, C., Guay, R., 1995. WinRHlZOTM, a Root-measuring system with a unique overlap correction method. HortScience 30, 906D–906.
Attia, H., Ouhibi, C., Ellili, A., Msilini, N., Bouzaïen, G., Karray, N., Lachaâl, M., 2011. Analysis of salinity effects on basil leaf surface area, photosynthetic activity, and growth. Acta Physiologiae Plantarum 33, 823–833.
Bekhradi, F., Delshad, M., Marín, A., Luna, M.C., Garrido, Y., Kashi, A., Babalar, M., Gil, M.I., 2015. Effects of salt stress on physiological and postharvest quality characteristics of different Iranian genotypes of basil. Horticulture, Environment, and Biotechnology 56, 777–785.
Bernstein, N., Kravchik, M., Dudai, N., 2010. Salinity-induced changes in essential oil, pigments and salts accumulation in sweet basil (*Ocimum basilicum*) in relation to alterations of morphological development. Annals of Applied Biology 156, 167–177.
Bilyera, N., Kuzyakova, I., Guber, A., Razavi, B.S., Kuzyakov, Y., 2020. How "hot" are hotspots: statistically localizing the high-activity areas on soil and rhizosphere images. Rhizosphere 16, 100259.
Bilyera, N., Kuzyakov, Y., 2024. Soil zymography: a decade of rapid development in microbial hotspot imaging. Soil Biology and Biochemistry 189, 109264.
Bunt, A.C., 1974. Some physical and chemical characteristics of loamless pot-plant substrates and their relation to plant growth. In: Acta Horticulturae. International Society for Horticultural Science (ISHS), Leuven, Belgium, pp. 1954–1965.
Caldwell, B.A., 2005. Enzyme activities as a component of soil biodiversity: a review. Pedobiologia 49, 637–644.
Caron, J., Rivière, L.M., Parent, L.E., Ilnicki, P., 2003. Quality of peat substrates for plants grown in containers. In: Parent, L.E., Ilnicki, P. (Eds.), Organic Soils and Peat Materials for Sustainable Agriculture, first ed. CRC Press, Boca Raton, pp. 67–92.
Cesbron, F., Metzger, E., Launeau, P., Deflandre, B., Delgard, M.-L., Thibault de Chanvalon, A., Geslin, A., Geslin, E., Anschutz, P., Jézéquel, D., 2014. Simultaneous 2D imaging of dissolved iron and reactive phosphorus in sediment porewaters by thin-film and hyperspectral methods. Environmental Science & Technology 48, 2816–2826.
Chaparro, J.M., Sheflin, A.M., Manter, D.K., Vivanco, J.M., 2012. Manipulating the soil microbiome to increase soil health and plant fertility. Biology and Fertility of Soils 48, 489–499.
Comerford, N.B., 2005. Soil factors affecting nutrient bioavailability. In: Bassiri Rad, H. (Ed.), Nutrient Acquisition by Plants: an Ecological Perspective, Ecological Studies. Springer, Berlin, Heidelberg, pp. 1–14.
Darrah, P., 1993. The rhizosphere and plant nutrition - a quantitative approach. Plant and Soil 155, 1–20.
Davison, W., Fones, G., Grime, G., 1997. Dissolved metals in surface sediment and a microbial mat at 100-μm resolution. Nature 387, 885–888.
Davison, W., Grime, G., Morgan, J., Clarke, K., 1991. Distribution of dissolved iron in sediment pore waters at submillimetre resolution. Nature 352, 323–325.
DeKalb, C.D., Kahn, B.A., Dunn, B.L., Payton, M.E., Barker, A.V., 2014. Substitution of a soilless medium with yard waste compost for basil transplant production. HortTechnology 24, 668–675.
Ge, T., Wei, X., Razavi, B.S., Zhu, Z., Hu, Y., Kuzyakov, Y., Jones, D.L., Wu, J., 2017. Stability and dynamics of enzyme activity patterns in the rice rhizosphere: effects of plant growth and temperature. Soil Biology and Biochemistry 113, 108–115.
Guber, A., Kravchenko, A., 2024. 2-D soil zymography: accounting for the spatial variation of pH. Rhizosphere 29, 100862.
Guber, A., Kravchenko, A., Razavi, B.S., Uteau, D., Peth, S., Blagodatskaya, E., Kuzyakov, Y., 2018. Quantitative soil zymography: mechanisms, processes of substrate and enzyme diffusion in porous media. Soil Biology and Biochemistry 127, 156–167.
Hinsinger, P., 1998. How do plant roots acquire mineral nutrients? Chemical processes involved in the rhizosphere. Advances in Agronomy 64, 225–265.
Hummel, C., Boitt, G., Santner, J., Lehto, N.J., Condron, L., Wenzel, W.W., 2021. Co-occurring increased phosphatase activity and labile P depletion in the rhizosphere of Lupinus angustifolius assessed with a novel, combined 2D-imaging approach. Soil Biology and Biochemistry 153, 107963.
Jézéquel, D., Brayner, R., Metzger, E., Viollier, E., Prévot, F., Fiévet, F., 2007. Two-dimensional determination of dissolved iron and sulfur species in marine sediment pore-waters by thin-film based imaging. Thau lagoon (France). Estuarine. Coastal and Shelf Science, Biogeochemical and contaminant cycling in sediments from a human impacted coastal lagoon 72, 420–431.
Jian, S., Li, J., Chen, J., Wang, G., Mayes, M.A., Dzantor, K.E., Hui, D., Luo, Y., 2016. Soil extracellular enzyme activities, soil carbon and nitrogen storage under nitrogen storage under nitrogen fertilization: a meta-analysis. Soil Biology and Biochemistry 101, 32–43.
Keeney, D.R., Nelson, D.W., 1982. Nitrogen—Inorganic forms. In: Page, A.L. (Ed.), Methods of Soil Analysis. Part 2. Chemical and Microbiological Properties, first ed., Agronomy Monographs. American Society of Agronomy, Inc., Soil Science Society of America, Inc., Madison, Wisconsin USA, pp. 643–698.
Knight, T.R., Dick, R.P., 2004. Differentiating microbial and stabilized β-glucosidase activity relative to soil quality. Soil Biology and Biochemistry 36, 2089–2096.
Koller, M., Alföldi, T., Siegrist, M., Weibel, F., 2004. A comparison of plant and animal-based fertiliser for the production of organic vegetable transplants. In: Acta Horticulturae. International Society for Horticultural Science (ISHS), Leuven, Belgium, pp. 209–215.
Kreuzeder, A., Santner, J., Prohaska, T., Wenzel, W.W., 2013. Gel for simultaneous chemical imaging of anionic and cationic solutes using diffusive gradients in thin films. Analytical Chemistry 85, 12028–12036.
Kreuzeder, A., Santner, J., Scharsching, V., Oburger, E., Hoefer, C., Hann, S., Wenzel, W. W., 2018. In situ observation of localized, sub-mm scale changes of phosphorus biogeochemistry in the rhizosphere. Plant and Soil 424, 573–589.
Kuzyakov, Y., Blagodatskaya, E., 2015. Microbial hotspots and hot moments in soil: concept & review. Soil Biology and Biochemistry 83, 184–199.
Kuzyakov, Y., Razavi, B.S., 2019. Rhizosphere size and shape: temporal dynamics and spatial stationarity. Soil Biology and Biochemistry 135, 343–360.
Kuzyakov, Y., Xu, X., 2013. Competition between roots and microorganisms for nitrogen: mechanisms and ecological relevance. New Phytologist 198, 656–669.
Liu, S., Razavi, B., Su, X., Maharjan, M., Zarebanadkouki, M., Blagodatskaya, E., Kuzyakov, Y., 2017. Spatio-temporal patterns of enzyme activities after manure application reflect mechanisms of niche differentiation between plants and microorganisms. Soil Biology and Biochemistry 112, 100–109.
Ma, X., Razavi, B.S., Holz, M., Blagodatskaya, E., Kuzyakov, Y., 2017. Warming increases hotspot areas of enzyme activity and shortens the duration of hot moments in the root detritusphere. Soil Biology and Biochemistry 107, 226–233.
Ma, X., Zarebanadkouki, M., Kuzyakov, Y., Blagodatskaya, E., Pausch, J., Razavi, B.S., 2018. Spatial patterns of enzyme activities in the rhizosphere: effects of root hairs and root radius. Soil Biology and Biochemistry 118, 69–78.
Mantelin, S., Touraine, B., 2004. Plant growth-promoting bacteria and nitrate availability: impacts on root development and nitrate uptake. Journal of Experimental Botany 55, 27–34.
Marschner, P., Marhan, S., Kandeler, E., 2012. Microscale distribution and function of soil microorganisms in the interface between rhizosphere and detritusphere. Soil Biology and Biochemistry 49, 174–183.
Matimati, I., Verboom, G.A., Cramer, M.D., 2014. Nitrogen regulation of transpiration controls mass-flow acquisition of nutrients. Journal of Experimental Botany 65, 159–168.
Metzger, E., Barbe, A., Cesbron, F., Thibault de Chanvalon, A., Jauffrais, T., Jézéquel, D., Mouret, A., 2019. Two-dimensional ammonium distribution in sediment pore waters using a new colorimetric diffusive equilibration in thin-film technique. Water Research X 2, 100023.
Metzger, E., Thibault de Chanvalon, A., Cesbron, F., Barbe, A., Launeau, P., Jézéquel, D., Mouret, A., 2016. Simultaneous Nitrite/Nitrate imagery at millimeter scale through the water–sediment interface. Environmental Science & Technology 50, 8188–8195.
Miranda, K.M., Espey, M.G., Wink, D.A., 2001. A rapid, simple spectrophotometric method for simultaneous detection of nitrate and nitrite. Nitric Oxide: Biology and Chemistry 5, 62–71.
Moorcroft, M.J., Davis, J., Compton, R.G., 2001. Detection and determination of nitrate and nitrite: a review. Talanta 54, 785–803.
Moran, J., McGrath, C., 2021. Comparison of methods for mapping rhizosphere processes in the context of their surrounding root and soil environments. Biotechniques 71, 604–614.
Murphy, J., Riley, J.P., 1962. A modified single solution method for the determination of phosphate in natural waters. Analytica Chimica Acta 27, 31–36.
Nannipieri, P., Trasar-Cepeda, C., Dick, R.P., 2018. Soil enzyme activity: a brief history and biochemistry as a basis for appropriate interpretations and meta-analysis. Biology and Fertility of Soils 54, 11–19.
Nguyen, C., 2003. Rhizodeposition of organic C by plants: mechanisms and controls. Agronomie 23, 375–396.
Paillat, L., Cannavo, P., Barraud, F., Huché-Thélier, L., Guénon, R., 2020. Growing medium type affects organic fertilizer mineralization and CNPS microbial enzyme activities. Agronomy 10, 1955.
Pausch, J., Kuzyakov, Y., 2011. Photoassimilate allocation and dynamics of hotspots in roots visualized by 14C phosphor imaging. Journal of Plant Nutrition and Soil Science 174, 12–19.
Pii, Y., Mimmo, T., Tomasi, N., Terzano, R., Cesco, S., Crecchio, C., 2015. Microbial interactions in the rhizosphere: beneficial influences of plant growth-promoting rhizobacteria on nutrient acquisition process. A review. Biology and Fertility of Soils 51, 403–415.

Plante, A.F., Stone, M.M., McGill, W.B., 2015. The metabolic physiology of soil microorganisms. In: Paul, E.A. (Ed.), Soil Microbiology, Ecology and Biochemistry, fourth ed. Academic Press. Elsevier, Boston, pp. 245–272.

Putievsky, E., 1983. Temperature and daylength influences on the growth and germination of sweet basil and oregano. Journal of Horticultural Science 58, 583–587.

R Core Team, 2020. R: a Language and Environment for Statistical Computing. R Foundation for Statistical Computing, Vienna, Austria. URL. https://www.R-project.org/.

Ren, C.J., Zhou, Z.H., Guo, Y.X., Yang, G.H., Zhao, F.Z., Wei, G.H., 2021. Contrasting patterns of microbial community and enzyme activity between rhizosphere and bulk soil along an elevation gradient. Catena 196, 104921.

Richardson, A.E., Barea, J.-M., McNeill, A.M., Prigent-Combaret, C., 2009. Acquisition of phosphorus and nitrogen in the rhizosphere and plant growth promotion by microorganisms. Plant and Soil 321, 305–339.

Sane, P., Agrawal, R., 2017. Pixel normalization from numeric data as input to neural networks: for machine learning and image processing. In: Proceedings of the International Conference on Wireless Communications, Signal Processing and Networking (WiSPNET), pp. 2221–2225. Chennai, India, 22 March 2017.

Santner, J., Zhang, H., Leitner, D., Schnepf, A., Prohaska, T., Puschenreiter, M., Wenzel, W.W., 2012. High-resolution chemical imaging of labile phosphorus in the rhizosphere of *Brassica napus* L. cultivars. Environmental and Experimental Botany 77, 219–226.

Santner, J., Larsen, M., Kreuzeder, A., Glud, R.N., 2015. Two decades of chemical imaging of solutes in sediments and soils – a review. Analytica Chimica Acta 878, 9–42.

Schindelin, J., Arganda-Carreras, I., Frise, E., Kaynig, V., Longair, M., Pietzsch, T., Preibisch, S., Rueden, C., Saalfeld, S., Schmid, B., Tinevez, J.-Y., White, D.J., Hartenstein, V., Eliceiri, K., Tomancak, P., Cardona, A., 2012. Fiji: an open-source platform for biological-image analysis. Nature Methods 9, 676–682.

Sinsabaugh, R.L., Lauber, C.L., Weintraub, M.N., Ahmed, B., Allison, S.D., Crenshaw, C., Contosta, A.R., Cusack, D., Frey, S., Gallo, M.E., Gartner, T.B., Hobbie, S.E., Holland, K., Keeler, B.L., Powers, J.S., Stursova, M., Takacs-Vesbach, C., Waldrop, M. P., Wallenstein, M.D., Zak, D.R., Zeglin, L.H., 2008. Stoichiometry of soil enzyme activity at global scale. Ecology Letters 11, 1252–1264.

Song, B., Razavi, B.S., Pena, R., 2022. Contrasting distribution of enzyme activities in the rhizosphere of European beech and Norway spruce. Front. Plant Sci. 13, 987112.

Spohn, M., Ermak, A., Kuzyakov, Y., 2013. Microbial gross organic phosphorus mineralization can be stimulated by root exudates – a 33P isotopic dilution study. Soil Biology and Biochemistry 65, 254–263.

Spohn, M., Kuzyakov, Y., 2013. Phosphorus mineralization can be driven by microbial need for carbon. Soil Biology and Biochemistry 61, 69–75.

Spohn, M., Kuzyakov, Y., 2014. Spatial and temporal dynamics of hotspots of enzyme activity in soil as influenced by living and dead roots—a soil zymography analysis. Plant and Soil 379, 67–77.

Spohn, M., Treichel, N.S., Cormann, M., Schloter, M., Fischer, D., 2015. Distribution of phosphatase activity and various bacterial phyla in the rhizosphere of Hordeum vulgare L. depending on P availability. Soil Biology and Biochemistry 89, 44–51.

Thibault de Chanvalon, A., Metzger, E., Mouret, A., Cesbron, F., Knoery, J., Rozuel, E., Launeau, P., Nardelli, M.P., Jorissen, F.J., Geslin, E., 2015. Two-dimensional distribution of living benthic Foraminifera in anoxic sediment layers of an estuarine mudflat (Loire estuary, France). Biogeosciences 12, 6219–6234.

Voroney, R.P., Heck, R.J., 2015. The soil habitat. In: Paul, E.A. (Ed.), Soil Microbiology, Ecology, and Biochemistry, fourth ed. Academic Press. Eldor A, Paul, Boston, pp. 14–40.

Wang, B., Yang, W., McKittrick, J., Meyers, M.A., 2016. Keratin: structure, mechanical properties, occurrence in biological organisms, and efforts at bioinspiration. Progress in Materials Science 76, 229–318.

Zhang, Y., Huang, W., Hayashi, C., Gatesy, J., McKittrick, J., 2018. Microstructure and mechanical properties of different keratinous horns. Journal of the Royal Society Interface 15.

Zheljazkov, V.D., Callahan, A., Cantrell, C.L., 2008. Yield and oil composition of 38 basil (*Ocimum basilicum* L.) accessions grown in Mississippi. Journal of Agricultural and Food Chemistry 56, 241–245.